Mine Water Environ (2016) 35:29–43
DOI 10.1007/s10230-015-0330-z

TECHNICAL ARTICLE

Tracing the Origin and Evolution of Geochemical Characteristics of Waters from the Candiota Coal Mine Area (Southern Brazil): Part I

C. Roisenberg · M. Loubet · M. L. Formoso · G. Berger · M. Munoz · N. Dani

Received: 17 March 2014 / Accepted: 5 February 2015 / Published online: 1 March 2015

Abstract This work correlates surface and ground water composition to the substrata, and traces how water chemistry evolves at Brazil's largest coal mine, the Candiota Mine. The water is dominated by SO_4, Fe, Ca, and Mg. A pH range of 2.7–3 in the pit lakes is attributed through chemical models to concomitant pyrite oxidation and carbonate dissolution along with slow hydrolysis of aluminosilicate minerals and buffering provided by several iron oxy-hydroxide species. The Fe deficit of the surface water relative to the expected values is mainly due to precipitation of Fe sulfate salts, hydroxysulfates, and oxyhydroxides in the waste piles and their runoff. A progressive decrease in oxygen partial pressure with increased lake depth leads to destabilization of the iron oxyhydroxides/hydroxysulfates formed near the surface, which explains their absence from the lake sediment. Although interacting with similar rock types, the groundwater has a significantly different composition than the surface water, with less salinity and a pH of 5–6.5, due to limited oxygen and its evolution in a nearly closed system that stabilizes at higher pH values, which is controlled by carbonate/bicarbonate buffering.

Keywords Acid mine drainage (AMD) · Water–rock interaction · Hydrogeochemistry · Geochemical modeling · Brazilian coal mine

Introduction

Oxidation of sulfides in mining areas can generate acidic, sulfate-rich acid mine drainage (AMD), with concurrent mobilization of various cations, including potentially toxic metals and metalloids (Casiot et al. 2003, 2009; Sánchez España et al. 2011). The process involves a great number of reactions, including: gas exchange, surface chemistry, aqueous complexation, redox reactions catalyzed by microbes, and formation of secondary minerals (Alpers et al. 1994; Hammastrom et al. 2005; Jambor 1994). AMD can thus affect the quality of ground and surface waters, as shown by many studies, e.g. Braungardt et al. 2003; Casiot et al. 2009; Elbaz-Poulichet et al. 1999, 2001; Nordstrom and Alpers 1999; Sánchez España et al. 2005a, b). The interaction of this acidic water with materials such as carbonates, silicates, or coal ash modifies their composition, often rendering them less acidic (Nicholson et al. 1988, 1990). Thus, the composition of surface water partially reflects the composition of the substrata, but mostly the composition and specific mineralogy of the materials on and near the mine surface. It also depends on the physical characteristics of these materials: their arrangement at the surface can hasten or slow the air- or water-facilitated oxidation process and interactions with other materials (Salomons 1995). These factors are a function of the

Electronic supplementary material The online version of this article (doi:10.1007/s10230-015-0330-z) contains supplementary material, which is available to authorized users.

C. Roisenberg (✉) · M. L. Formoso · N. Dani
Instituto de Geociências, Univ Federal do Rio Grande do Sul (UFGRS), 9500 Bento Gonçalves ave, Porto Alegre 91501-970, Brazil
e-mail: claroi@aim.com

M. Loubet · M. Munoz
Géosciences Environnement Toulouse (GET), Univ Toulouse III - UMR 5563 - UR 154 CNRS - IRD - OMP, 14 Edouard Belin ave, 31400 Toulouse, France

G. Berger
CNRS, IRAP, 14 ave, Edouard Belin, 31400 Toulouse, France

geological, hydrological, and climatological environment, and the geometry of exploitation, and thus are, to some degree, mine specific.

We focus here on the Candiota coal mine in southern Brazil. Previous studies have highlighted the degradation of water quality in streams impacted by coal mining in the Candiota region, as reflected by low pH and a significant increase in SO_4 and some metals, including Fe, Mn, Al, Ni, Zn, Cd, and Hg (Fiedler and Solari 1988; Fiedler et al. 1990; Machado 1985; Machado et al. 1984; Martins and Zanella 1987, 1990; Streck 2001). Teixeira et al. (2000) reported that metals are mainly transported in these streams as suspended matter. Very few geochemical studies report on the surface water of the Candiota mine itself (Martins and Zanella 1987). Data on the groundwater composition of the Candiota region are also scarce, though elevated cation content has been noted in some wells in this region (Machado et al. 1984). However, all of these Candiota studies remain partial and lack a global analysis of the water quality degradation from coal mining.

This study was developed to provide that global perspective, with two main goals, to: (1) assemble a large set of physicochemical data on surface water (including drainage water from the waste piles, retention lakes, and streams) and groundwater from the Candiota mine, which will allow an evaluation of the influence of mining activities; (2) describe the processes leading to the initial geochemical characteristics of the surface water and the evolution of this water over space and time. To do this, we analyzed a large amount of material in addition to surface- and ground-water samples, including substratum rocks, mine spoil, alteration products, and precipitates. Leaching experiments were also carried out on various materials and the resulting solutions were compared with the surface water.

We normalized the water composition to a mean composition of substratum rocks affected by the weathering process. This methodology can indicate how water chemistry reflects successive dissolution/oxidation reactions and subsequent evolution of the waters due to precipitation processes. Further constraints on the geochemical history of the waters resulted from analysis of specific water characteristics (i.e. pH constancy, elemental correlations, and evolution of some elements relative to SO_4 displaying a conservative behavior). Finally, in light of geochemical modeling and thermodynamic considerations, we propose water genesis and evolution pathways summarized in a mass balance synthesis that considers the dissolution/precipitation of specific minerals that affect the surface water chemistry and fits our mineralogical observations.

Study Site

The Candiota area, located in the southwestern portion of the Rio Grande do Sul State, includes Brazil's largest coal reserve, with proven reserves of 1.7 billion tonnes (DNPM 2006). Coal in Rio Grande do Sul (Fig. 1) is encased in the Rio Bonito Formation, an interbedded fluvial to marine sandstone, mudstone, and coal lithostratigraphic unit deposited in paralic environments (deltaic, estuarine, and shallow marine) during the early Permian (268–258 Ma; Daemon and Marques-Toigo 1991). Based on regional sequence stratigraphic analysis, the coal was formed in a back barrier depositional setting (Holz 1998) composed of arborescent and herbaceous plant material that accumulated under cold and humid conditions (Patzkowsky et al. 1991). The Rio Bonito coal zone consists of estuarine and shallow marine sandstone intercalated with coal seams (Holz and Kalkreuth 2004). Major coal development is associated with the lower sequence in a transgressive systems tract (Fig. 1). Diagenesis of coal resulted in extensive formation of concretionary pyrite, and strata-bound calcite and kaolinite in sandstone in the vicinity of parasequence boundaries with coal layers (Ketzer et al. 2003).

More than 20 coal seams have been found in the Candiota Mine, but only the Lower and Upper Candiota coal seams (LCS and UCS) are of economic interest and currently mined for electric power generation. These seams are approximately 2.5 m thick and are separated by a clay layer 1 m thick, 20–30 m below the surface. The Candiota mine extends across an area of 430 km^2 and includes two abandoned mined areas: one closed in 1974 (Malha I) and the other in 1990 (Malha II). At present, there are two active mines (Malha IV and VII), both of which have employed strategic land restoration. After burning at the Presidente Medici thermoelectric plant, coal ash is returned to the Candiota mine and placed between the reject piles, restoring the original topography. Mining has led to the formation of small artificial pit lakes that will later be engulfed by reject piles. These lakes are used as decanting areas that limit the flow of water and sediment into adjacent streams.

Materials and Methods

Sampling and Analytical Procedures

Water samples were mainly collected during two campaigns: the first in December 2004 during the dry season and the second in May 2005 during the rainy season (after 3 days of rainfall). Additional sampling was performed in October 2006. Four water compartments were sampled

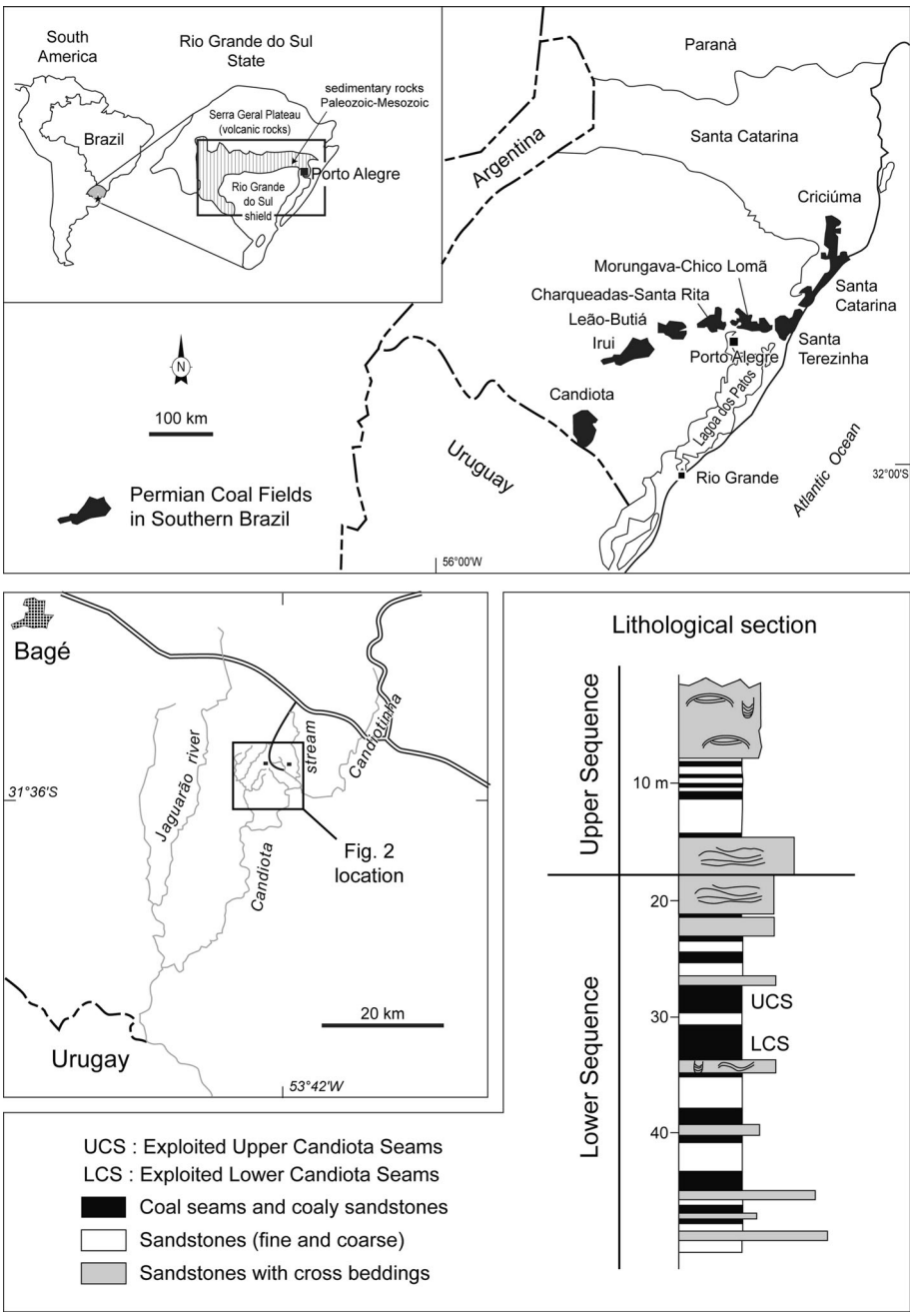

Fig. 1 Location of the Candiota Mine in the southern Brazil Permian coalfields, and a typical lithological log with the main coal seams shown

(Fig. 2): (1) pit lake waters from distinct mining areas (Malha I, II, IV)—L1 (L1A and L1B), L2 (L2A, L2B and L2C), L4 (L4A and L4B); (2) mine waste piles runoff from two mining areas (Malha II and IV)—P2 and P4 (P4A and P4B); (3) stream waters sampled from the Candiota area (SA, SB, SC), and water from a puddle within the coal stock area (DEC, SD). The sampled streams issued from mining areas, except SB, which issued from unexploited areas and can be considered the 'natural geochemical background' of the Candiota area. Lastly (4) groundwater was sampled from different levels of four distinct piezometers (boreholes H_A, H_B, H_C, H_D).

Water samples collected for cation determination were filtered on site through a 0.22 µm Millipore membrane (using a Sartorius polycarbonate filter holder and nitrate cellulose Sartorius single-use filters with a 47 mm diameter) using a manual vacuum pump. The first 250 mL of the filtrate was systematically rejected. Filtered solutions were acidified to pH = 1 with ultrapure double-distilled 12N HNO_3 for later analysis of cations and trace elements. Samples were stored in polypropylene containers previously washed with 2N distilled HCl solution and rinsed with MilliQ deionized water. Water samples collected for alkalinity and anion determinations were filtered but not

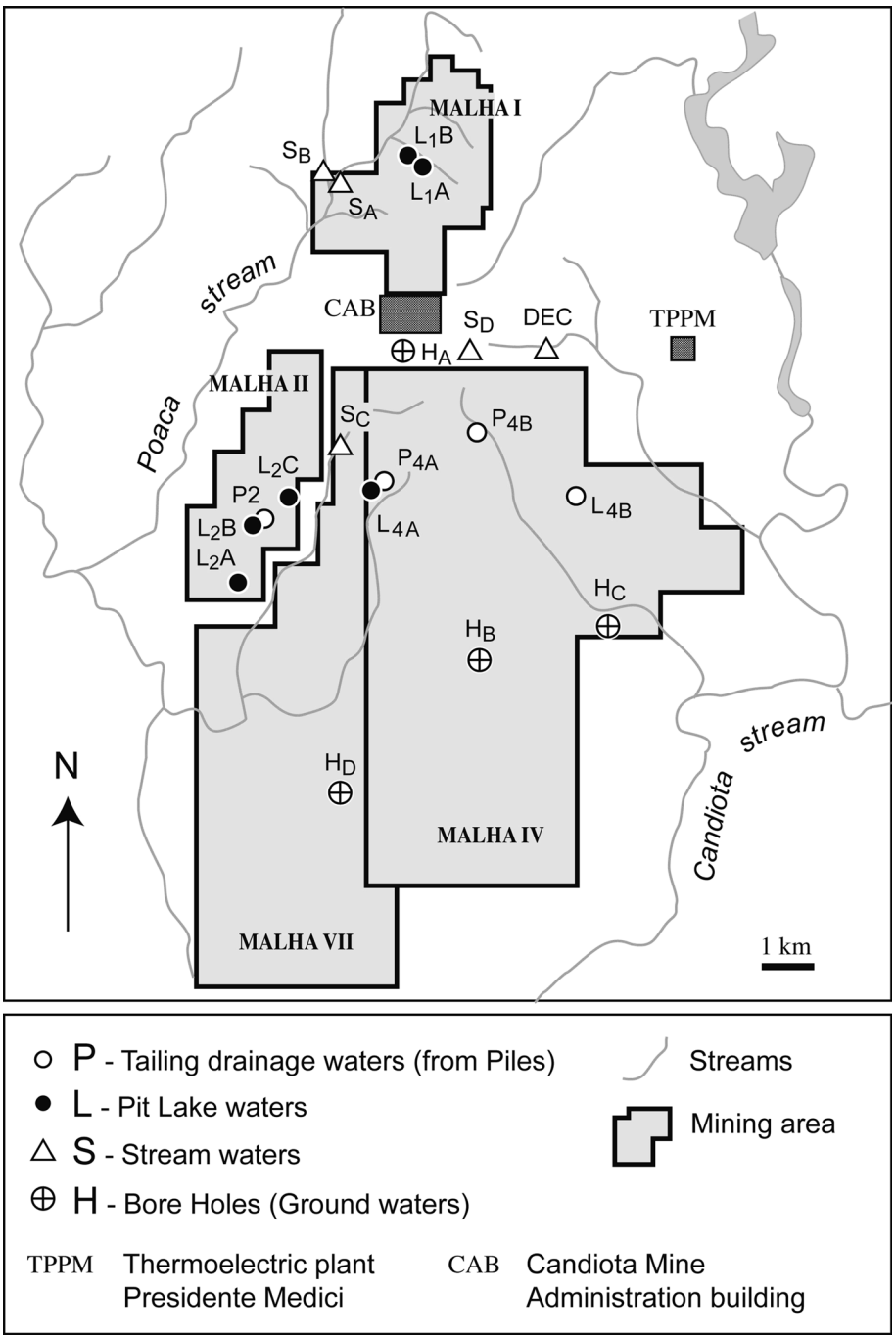

Fig. 2 Schematic sampling location of the Candiota mine showing distinct exploited areas (*Malha I, II, IV, VII*) and distinct water samples collected from piles, pit lakes, streams, and bore holes

acidified. Blank tests were performed during the sampling campaign to determine possible contamination due to the filtration and storage protocols. For major elements, as for most trace elements, very low blanks were found (compared with river water contents).

The pH, Eh, and electrical conductivity (EC)/TDS were measured in the field. Analyses for dissolved cations were performed at the GET laboratory (Toulouse, France), using an inductively coupled plasma mass spectrometer (ICP-MS, Perkin-Elmer Elan 6000) and an atomic absorption spectrometer (AAS, Perkin-Elmer 5100 ZL), with an air-C_2H_2 gaseous mixture. Anions were identified by high performance liquid chromatography (HPLC, Dionex D300); alkalinity was determined with an automatic titrator (Schott Titrolab 96), with 0.01N hydrochloric acid (Gran method). Analytical results are listed in Supplemental Table 1. Supplemental files accompany the on-line version of papers, which can be downloaded for free by all IMWA members and journal subscribers.

The collected solid samples comprised substratum rocks, mine waste solids, and coal ash collected at the mine surface, sandstone from drill core H_C, and sediment

samples collected at the bottom of lakes and streams. To identify the mineralogical forms and associations in these solid materials, thin sections and x-ray diffraction (XRD) analyses were conducted at the UFRGS laboratory (Porto Alegre, Brazil). XRD was performed on random and oriented powders (<20 and <2 μm fractions). Air-dried, ethylene glycol-solvated, and heated (calcinated, 550 °C, 2 h) samples were examined in a Siemens D-500 diffractometer using CuKα radiation.

Total extraction was performed on solid samples using $HNO_3 + HF + H_2O_2$ digestion, and was analyzed by AAS, ICP-MS (GET laboratory), and X-ray fluorescence (UFRGS laboratory—Rigaku RIX 2000). To simulate the weathering of materials from the Candiota surface mining area, leaching experiments were performed on the coals, coal ash, and sandstone samples. These experiments were conducted using 15 mL 0.01N nitric acid stirred for 24 h with a 0.1 g mass of sample. Solutions were centrifuged and 10 mL was removed for analysis by AAS and ICP-MS. Although sulfate acidic solutions would also be a valuable simulation of interaction processes occurring in Candiota, they were discarded due to precipitation of sulfate-bearing minerals.

Geochemical Modeling

PHREEQC geochemical modeling software (Pankhurst and Appelo 1999, version 2.15.0, Feb. 5, 2008) was used to calculate (1) activity coefficients, (2) ionic speciation, and (3) saturation indices (SI) for all the phases of the data base. It was also used to simulate the evolution of composition of a given solution in equilibrium with mineralogical assemblages from the Candiota mining area and predict the nature and extent of secondary phases formed along this evolution. The thermodynamic data base of PHREEQC 2.15.0 was enlarged with data from Bigham et al. (1996) to include the solubility of schwertmannite.

Results

Mineralogy of Sandstones, Coal, and Coal Ash Interacting with Surface Waters

Thin section descriptions and XRD analyses (Supplemental Table 2) allowed precise petrographic and mineralogic characterization of the materials exposed at the surface. The following description takes into account recent analyses and previous descriptions made by other groups (Correa da Silva 1993; Kalkreuth et al. 2006; Ketzer et al. 2003).

The dominant sandstone in waste rock piles is mainly medium- to fine-grained subarkose to quartz arenite. Minerals of detritic origin include quartz grains (dominantly monocrystalline) and K-feldspar, which dominates over plagioclase and kaolinite. Micas (biotite and muscovite), heavy minerals (tourmaline, epidote, zircon, and garnet), opaque minerals, and glauconite are only minor components. The mineral assemblage of diagenetic origin is composed of kaolinite, chlorite, pyrite, calcite, siderite, ankerite, and anhydrite. Pyrite is common (<20 vol %) and occurs mainly as centimetric concretions in microcrystalline and blocky forms. Calcite occurs as pore-filling cement (<15 vol %) in microcrystalline, poikilotopic, and mosaic forms closely associated with pyrite concretions. Kaolinite is common in sandstones (<10 vol %) and fills intergranular pores or replaces mica and feldspar. The spatial distribution of diagenesis is mainly controlled by stratigraphy. Pyrite concretions, stratabound calcite, and kaolinite occur in sandstones above and below coal layers of parasequence boundaries (Ketzer et al. 2003).

The Candiota coal reflectance (0.41–0.52 %) is indicative of subbituminous rank with high mineral matter content (<30 vol %), which includes clay minerals (kaolinite, smectite, chlorite; <10 vol %), sulfides (pyrite, marcasite; <10.5 vol %), silicate minerals (quartz; <9 vol %), and carbonates (calcite, dolomite, siderite; <7 vol %). Total sulfur content ranges from 0.28 to 11.46 wt.%, due mostly to variations in pyrite.

The ashes are combustion by-products from the power plant (Table 2). Fly ash is composed of glassy aluminum–silicate matrix, mullite, quartz, and magnetite. Bottom ash has a similar composition, with a higher magnetite content (Pires and Querol 2004).

Pyrite oxidation is clearly observed in the field. The melanterite ($FeSO_4 \cdot 7H_2O$) detected by XRD analyses forms white acicular crystals that coat exposed coal and oxidized pyrite concretions in the sandstone in the mine spoils. This soluble iron sulfate salt is formed in the first stages of the alteration process or by an evaporative process (Sánchez España 2007), which explains why this mineral was only found locally. Less soluble than melanterite, gypsum was observed in the field under similar conditions (associated with pyrite concretions in sandstone and coal). Among the various oxy-hydroxides that should constitute alteration products of pyrite, goethite constitutes a common XRD-detected phase.

The mine spoil discharges show a variety of yellow–red colors related to nearly amorphous iron oxyhydroxides/hydroxisulfates precipitates, but were not always recognized by XRD analysis. Among these poorly crystallized

minerals, jarosite ($KFe_3(SO_4)_2(OH)_6$) was identified in just one mine waste sample. Schwertmannite ($Fe_8O_8(OH)_6SO_4$) is the likely dominant precipitate in AMD at pH 2–4, but was not detected by XRD, nor was ferrihydrite ($Fe_5HO_8 \cdot 4H_2O$), which commonly precipitates from mine waste effluents at a higher pH than schwertmannite (Bigham et al. 1996; Bigham and Nordstrom 2000; Sánchez España et al. 2005a).

Bottom lake deposits were found to be similar to sandstone and coal mineralogy, mainly composed of a mixture of detrital and diagenetic minerals: quartz, K-feldspar, mica, and kaolinite. According to their color, these materials appear to lack iron oxides or oxyhydroxides. Goethite (α-FeOOH) was identified in only one sample (BLD-L1A-II) that had formed under specific conditions (described later).

Table 1 Chemical composition of solid materials and leaching solutions

Sample	Ca ppm	Mg ppm	Na ppm	K ppm	Al ppm	Fe T ppm	Si ppm	Ti ppm	V ppm	Ga ppb	Ge ppb
Sandstones and siltstones from drill core HC											
HC-1	543	2257	670	17,523	88,079	59,817	n.m.	3183	128,374	30,877	2212
HC-2	117	318	1299	8069	15,711	47,133	n.m.	425	9291	4817	713
HC-3	128	462	368	6099	108,122	23,910	n.m.	594	19,062	12,073	1287
HC-4	84	115	3637	14,933	64,010	115,621	n.m.	291	5540	5072	2998
HC-5	221	2130	10,132	18,955	113,373	7791	n.m.	3609	98,515	23,966	688
HC-6	664	4132	4514	18,794	108,398	37,889	n.m.	6483	120,783	27,988	1168
HC-7	637	4993	627	36,835	100,292	120,916	n.m.	6263	160,906	37,334	1358
Massive coal from front mine											
Coal-1	1350	2356	588	8383	65,516	10,837	n.m.	2428	36,613	11,799	1233
Coal-2	*17,581*	*4221*	*2226*	*13,780*	*131,883*	*18,325*	*395,988*	n.m.	n.m.	n.m.	n.m.
Coal sample with pyrite level											
COAL-3	*90,838*	*2050*	*1484*	*1494*	*6933*	*455,123*	*71,838*	n.m.	n.m.	n.m.	n.m.
Sandstone with pyrite concretions											
PYR-Co	334	59	310	5952	5290	227,051	n.m.	110	1346	996	1453
Coal ash											
ASH-1	9557	4452	1535	12,288	84,672	41,859	n.m.	3742	81,252	23,850	3427
ASH-2	*16,295*	*6392*	*2077*	*14,694*	*110,556*	*31,615*	*421,108*	n.m.	n.m.	n.m.	n.m.
Bottom lake deposits (BLD) and bottom stream deposits (BSD)											
BLD-L1A-I	130	1244	337	4641	51,633	42,575	n.m.	3010	76,450	15,656	1554
BLD-L1A-II	*214*	*1387*	*890*	*8135*	*89,228*	*28,537*	*431,221*	n.m.	n.m.	n.m.	n.m.
BLD-L1B-I	113	433	444	9175	24,257	10,794	n.m.	1183	27,174	6902	1136
BLD-L2B-II	3149	4803	634	8845	58,310	18,729	n.m.	3233	74,758	18,940	1542
BSD-SC	423	2436	957	6869	62,553	49,038	n.m.	2996	69,864	19,328	1897
Precipitates from surface solutions (from P4B mine waste pile)											
P4B-I	*98,056*	*3738*	*74*	*8717*	*51,388*	*24,270*	*265,101*	n.m.	n.m.	n.m.	n.m.
P4B-II	*1572*	*2653*	*<0.1*	*4151*	*33,447*	*373,779*	*228,497*	n.m.	n.m.	n.m.	n.m.
P4B-VII	*2144*	*2472*	*<0.1*	*2656*	*14,342*	*377,766*	*111,900*	n.m.	n.m.	n.m.	n.m.
P4B-VIII	*4288*	*2653*	*1113*	*4317*	*16,406*	*389,027*	*109,942*	n.m.	n.m.	n.m.	n.m.
Leachates of solid materials											
ASH-1-Lch	28.6	0.9	0.7	1.2	5.9	7.2	5.1	0.16	41.2	5.00	7.99
PYR-Co-Lch	0.5	0.1	0.1	0.6	3.2	94.6	0.0	0.03	2.8	0.81	0.03
Coal-1-Lch	9.9	2.7	1.2	1.6	0.5	5.5	1.4	0.05	41.8	0.38	0.39
HC-1-Lch	7.1	2.9	0.3	1.0	0.8	0.1	4.2	0.00	0.1	0.32	0.07
BLD-L2B-II-Lch	29.5	11.7	0.1	1.2	1.8	4.2	2.4	0.01	5.7	0.27	0.24

Numbers in italics: X-ray fluorescence analysis (UFRGS laboratory, Porto Alegre); numbers in normal font: atomic absorption (Ca, Mg, Na, K, Al, Fe Total), ICP-MS analysis: Ti, V, Ga, Ge; colorimetric analysis of silica (GET laboratory, Toulouse)

n.m. not measured

Chemical Composition of Sandstones, Coal, and Coal Ash Interacting with Surface Waters

The major element chemical compositions of sandstone, coals, and coal ash samples from mine spoils (Table 1) were plotted in a conventional continental crust (CC)-normalized representation (Taylor and McLennan 1985), together with two trace elements (Ga and Ge) known to display close geochemical behavior with Al and Si major elements, respectively (Fig. 3). The CC-normalized spectra displayed by surface materials allows the definition of a reference spectrum corresponding to the mean compositional range of the solids found at the surface, referred to as MCSSW (mean composition of solids interacting with surface waters).

Sandstone, coal, and ash materials display closely parallel patterns (or spectra) with similar characteristics. The mean composition of these materials displays close CC compositions of Al (Ga), Si (Ge), Ti, and V, which are "lithophile type elements", and significant depletion of alkaline and calc-alkaline elements (Ca, Mg, Na, K) relative to the mean CC composition. Among these latter elements, Ca, Mg, and Na are more significantly depleted than K. The more variable behavior of the Fe in these materials is likely from Fe localization within pyrite grains and the distribution of these phases in localized concretions and strata.

Coal burning in a thermoelectric plant eliminates volatile compounds, leading to increased refractory elements concentrations in the ash. Thus, with the exception of volatile compounds, coal ash should display compositions close to the coal, taking into account an enrichment factor. This is actually the case for the elements in this representation, with enrichment factors of approximately 1 for Al, 1.2 for K, and 2.8 for Fe.

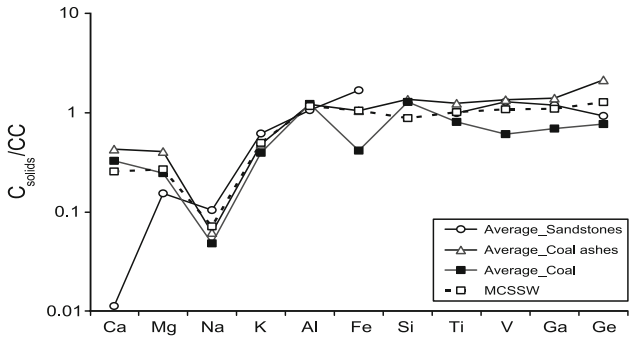

Fig. 3 Continental crust (CC)-normalized major element contents of coal, sandstone, and coal ash samples together with the CC-normalized contents of trace elements Ga, Ge displaying geochemical properties closely similar to Al and Si, respectively. *Patterns* shown are the average for each type of solid (coal, sandstone, and coal ash), and MCSSW corresponds to the Mean Composition of Solids interacting with Surface Waters. CC composition from Taylor and McLennan (1985)

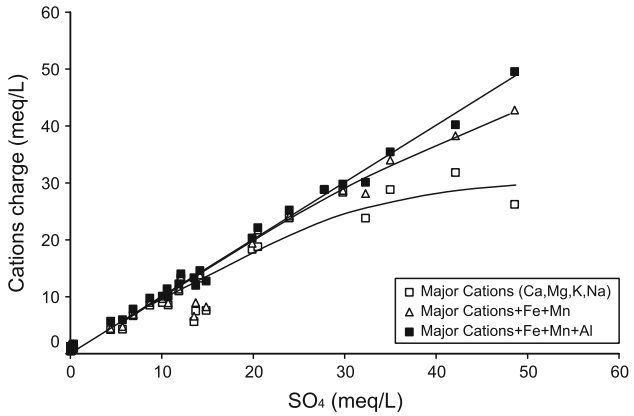

Fig. 4 Total charge of major cations in Candiota mine surface waters versus the sulfate charge

Surface Water Chemistry

Water composition analytical data confidence (Supplemental Table 1) is generally assessed by the normalized inorganic charge balance [NICB = (total cationic charge − total anionic charge)/total cationic charge], a term introduced by Stallard and Edmond (1983). As an example of the usefulness of this term, a study of imbalance in favor of positive charges (NICB > 0) of organic-rich river waters (Tosiani et al. 2004) was shown to be due to the presence of organic acids, whose dissociation produces H^+ and organic anions (the latter not measured in the analytical procedure). In computing this term, we considered the major components as 100 % present as simple ions, ignoring charges that may originate from sulfate complexes, as this would have needed more sophisticated computations and PHREEQC modeling for each element. Variations in NICB values may have resulted from this simplification. Nevertheless, the computed NICB values of the surface water samples were satisfactory, with many values significantly less than 5 % and the greatest being 22 % (sample L1A-a).

In surface waters, sulfate was the dominant anion, while Ca, Mg, and K represent the dominant cations, with a global charge balance (Fig. 4). Although mainly present in a simple ionic form, all of these ions were also partly (1–30 %) associated with sulfate complexes. Mine waste drainage waters were the most sulfate-enriched (up to 24.2 μmol/kg), and the most acidic (pH 2.2). In these cases, Fe was a prominent constituent (mostly as Fe^{2+} and partly as an $FeSO_4$ complex), followed by cations and sulfate complexes of Ca, Mg, and Al (Fig. 5).

Pit lake waters have a low pH (range 2.7–3.3) and their sulfate content extends over a very large range (tens to thousands of mg/L). They are less contaminated than most waste pile drainage water, and significantly worse than groundwater and unpolluted streams (Fig. 6). The high

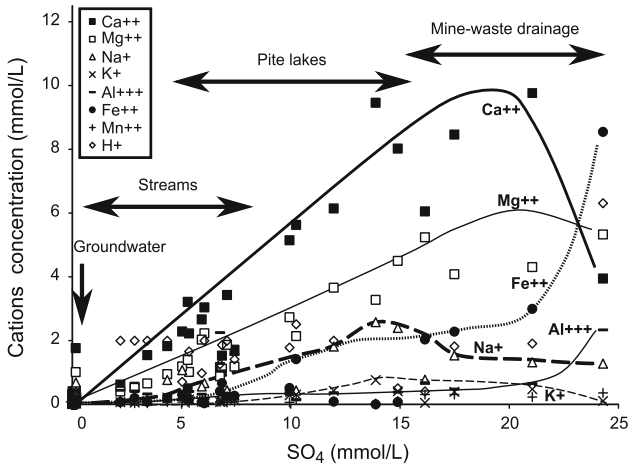

Fig. 5 Major cations contents of Candiota mine surface waters versus the SO_4 content

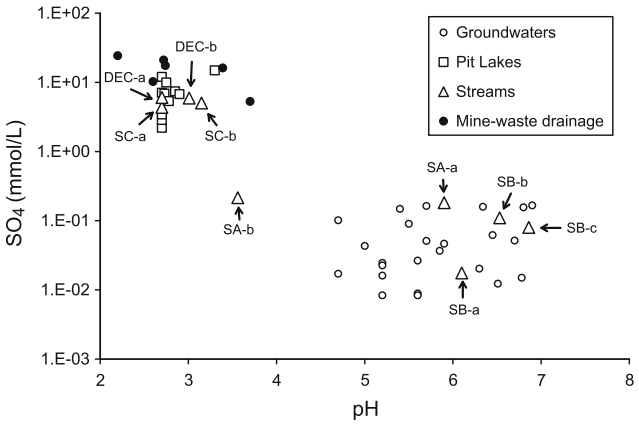

Fig. 6 SO_4 content versus pH of surface waters and groundwaters from Candiota mine showing the clear distinct composition. Note the uniform range of pH (approximately 2.7) of pit lake waters, the compositional range of stream waters, a function of their location in explored or unexplored areas of the mine, and distinct behavior of the SA stream water between the two campaign collections (see text for explanation)

sulfate concentration of pit lake water is balanced by Ca and Mg cations, displaying fairly constant Ca/SO_4 and Mg/SO_4 ratios. Although less impressive, a similar correlation also relates Na, K, and SO_4 content. Such correlations represent original features that will be discussed later. In contrast, Al and Fe do not follow such patterns and display a limited compositional range.

These surface water chemistry characteristics, with very low pH values and very high sulfate, are similar to those observed at other mining sites, e.g. AMD from abandoned underground coal mines in Central Montana (Gammons et al. 2010), pit lakes from the Iberian Pyrite Belt (Sánchez España et al. 2005b), and open pits at the Mount Morgan Au-Cu mine in Australia (Edraki et al. 2005). However, coal mine discharges displaying higher pH values are also classically observed in many areas, such as in some abandoned coal mines in Pennsylvania, which have a pH range of 2.7–7.3 (Cravotta 2008).

Stream waters display very distinct compositions depending on their origin and location. When issuing from mine waste (locations SC and DEC), stream waters display closely similar geochemical characteristics to surface water associated with mine waste elsewhere, typically with a very low pH ($\approx$2.7). In unexploited parts of the mine (i.e. SB), stream water displays less acidic or quasi-neutral compositions, with a pH ranging from 5.9 to 6.5, and are characterized by low major element contents (Fig. 6). Stream SA shows large seasonal variations, with a groundwater-like composition (type SB) in the dry season (sample SA-a) and a composition intermediate between groundwater and pit lakes in the rainy season (sample SA-b). These compositions indicate that the draining zone of this stream is limited to an unexploited area in the dry season but expands to an exploited area or includes stream contributions from such zones in the rainy season.

Groundwater Chemistry

Computed NICB values for most groundwater samples are less than 12 %, indicative of a good charge balance. The higher NICB values found in some samples should be ascribed to the relative measurement uncertainties of the very low major element content of these waters. Groundwater displays geochemical characteristics that clearly distinguish it from surface water, particularly a low cation and anion content (Fig. 5). Groundwater pH ranges from 4.7 to 7.4, and sulfate is not the dominant anion that balances the cationic charge, occurring in low amounts with nitrate and chloride (Fig. 7a). The percentage of bicarbonate is equivalent to other anions in the low pH range (pH $\approx$ 4.5), but becomes predominant with increasing pH. At high bicarbonate content, pH stabilizes at approximately 6.3–6.9 (Fig. 7b).

Discussion

Interpretation of Surface Water Chemistry

To develop an interpretation of surface water chemistry, some main characteristics of the Candiota waters, including the dissolution of elements from the substrata, elemental correlations, and pH stability, will be emphasized first. Analysis of these characteristics, as thermodynamic considerations, constrains the conditions of water genesis and evolution at the surface. Finally, mass balance budget modeling of water genesis through alteration and evolution at the surface will be developed to fit the surface water compositions.

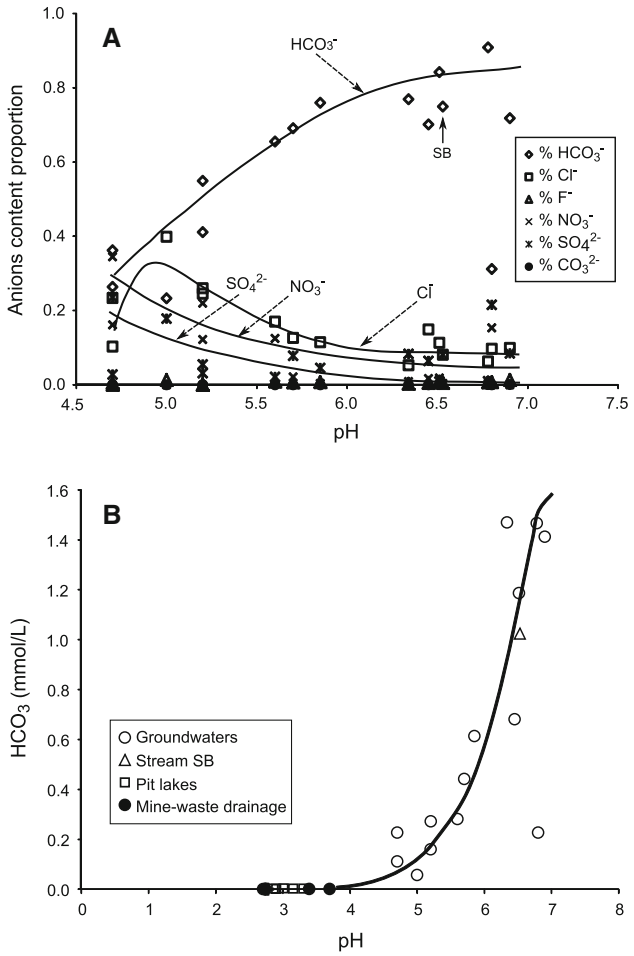

Fig. 7 **a** Anions content proportions (HCO_3^-, SO_4^-, NO_3^-, Cl^-) versus pH in Candiota mine groundwaters; **b** HCO_3^- mole content versus pH in the Candiota mine waters

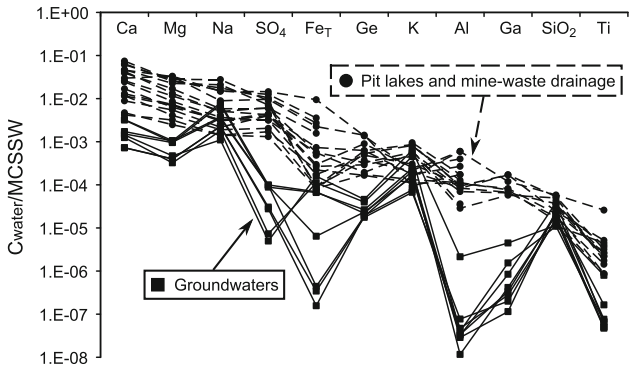

Fig. 8 MCSSW (mean composition of solids interacting with surface water) normalized compositions of groundwater and surface water (pit lakes and mine-waste waters) from Candiota mine. The lower compositional range of groundwaters relatively to surface waters is manifest

Geochemical Characteristics of Surface Waters

As mentioned previously, solid surface materials (sandstone, coal, and coal ash) display close CC-normalized patterns. The common origin of these materials explains their similar compositional characteristics. The sandstone and coal were deposited in an estuarine environment. In this environment, as in rivers, sediment from a detrital origin (sandstone) and suspended materials (clays) display similar depletions in alkali and calc-alkali elements (Dupre et al. 1996; Tosiani et al. 2004), and organic matter is partly sorbed and thus transported by suspended matter (Pérez et al. 2011).

The common characteristics of the Candiota surface solids retraced by the MCSSW spectrum reflect their relative elemental content, with CC-like ratios for some elements (Al, Si, V, Ga, Ge) and depletion factors relative to CC-like compositions (alkali and calc-alkali depletion) for others. The similar relative proportion of elements in these materials allows estimation of the fractionation processes along the alteration process from surface solids to water. Figure 8 presents the major cations content of pit lake water and groundwater normalized to the MCSSW. Sulfur fractionation from the surface solid materials to the lake waters was also computed by dividing the sulfate content of the pit lake water to a theoretical "sulfate equivalent sulfur" of the substratum material. Assuming that Fe and S are mainly controlled by pyrite in the solid materials, this theoretical sulfur content was estimated as twice the average Fe content in sandstone and coal.

From the surface water chemical characteristics in the previous paragraphs, and analysis of the MCSSW normalized surface water spectra, the main geochemical features can be outlined as follows:

1. The most important enriched elements in surface water with respect to substrata rock distributions were Ca, Mg, Na, and S (as SO_4). Consistently, the most important enriched elements in the leached solutions in laboratory experiments, relative to their distribution in the leached rocks, were Ca, Mg, and Na (Fig. 9). Ca and Mg enrichment in the surface water most likely originates from carbonates (calcite, siderite, ankerite) as well as plagioclase for Ca, mica for Mg, and pyrite for S (as SO_4). The less notable enrichment of Na and K, compared to these other elements, can be assigned to lower kinetics of plagioclase and K-feldspar dissolution, respectively.
2. A good correlation is noted in the pit lake waters between sulfate and Ca, Mg, and Na content. This correlation is demonstrated by parallel evolution of the MCSSW normalized surface water spectra. This correlation indicates that these elements should not be significantly involved in precipitation processes during surface water evolution.
3. Compared to the relative molar content of Fe and S in pyrite (the main source of these elements), Fe

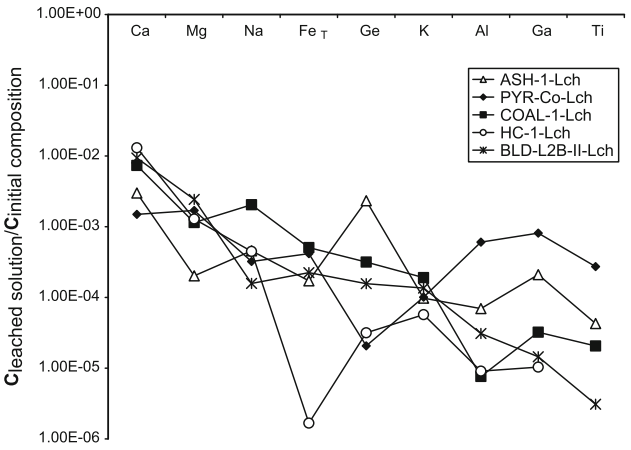

Fig. 9 Leaching experiments results: ratio of composition of leached solutions over initial composition of leached materials, for major elements and associated trace elements

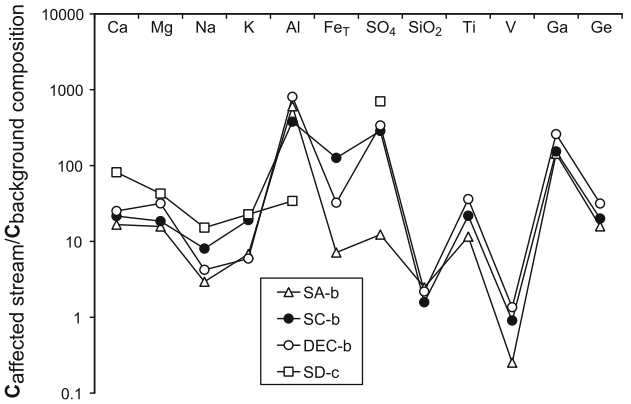

Fig. 10 Water composition of mine-affected streams normalized to the surface water background, corresponding to the composition of an unaffected stream (SB sample)

depletion relatively to S was observed in the surface water. This will be explicitly discussed later.

Streams issuing from unexploited areas can be used as a reference for the geochemical background of surface water in the Candiota area. Normalization of the mine-affected stream to background composition highlights SO_4, Fe, Ca, Mg, Na, K, Si, Ge, and Ti enrichment (Fig. 10), a result of active alteration processes. The more intense Al (and Ga) enrichment in the AMD waters relative to background results from the higher solubility of Al in acidic conditions.

Equilibrated Phases with Surface Waters: Silicates/Clay Minerals, Sulfate-Bearing Phases

SI calculations using PHREEQC were performed to assess mineral stability in surface water conditions. The silicate phases (plagioclase, K-feldspar, and mica), as well as pyrite and carbonate minerals (calcite, siderite, and ankerite) that constitute the primary mineralogical assemblage of the substratum rock, are significantly undersaturated, indicating their potential dissolution along the alteration process.

Surface waters, characterized by elevated sulfate concentrations, would be expected to reach equilibrium with some sulfate compounds. Modeling indicates positive SI values for several sulfate-bearing phases: barite ($BaSO_4$), jarosite ($KFe_3(SO4)_2(OH)_6$), alunite ($KAl_3(SO_4)_2(OH)_6$), and schwertmannite ($Fe_8O_8(OH)_{4.5}(SO_4)_{1.75}$, where x falls within 1–1.75) which are highly *pe* dependent (O_2 pressure sensitive). Modeling indicates their stability at low pH under oxidic conditions (surfaces of lakes and streams), favoring Fe^{3+} speciation in solution. Jarosite was observed in the field (in pile P4), as was alunite (one occurrence in a substratum rock), but not schwertmannite. Other sulfate-bearing phases, such as polyhalite ($K_2MgCa_2(SO4)_4{\cdot}2H_2O$) and syngenite ($K_2Ca(SO_4)_2{\cdot}2H_2O$) had negative SI values and were not observed. Oversaturation of melanterite was computed, in agreement with field observations. Slightly negative SI values (-0.2 to -0.6) were calculated for gypsum, indicating that it might precipitate locally, which was in fact observed. Gypsum precipitation should take place where calcite and pyrite are closely associated.

Under acidic conditions, few clay minerals are secondary stable products, according to the modeling. Kaolinite, a member of the primary mineralogical assemblage, had positive or near-zero SI, and was commonly observed in the field.

Fe Behavior: Speciation and Mineralogy

According to the Fe/S molar ratio in pyrite, without any scavenging of Fe, total Fe concentrations would be expected to be about half of the sulfate molar content (without sulfate precipitation). The cationic versus SO_4 molar content of the surface water shows that this is not the case. Fe content was approximately 1/3 of the expected value and even lower in many cases. Fe content increased in the very acidic mine waste pile water, but still did not reach the expected theoretical values.

Various forms of Fe speciation (in solution and solid phases) are highly redox- and pH-dependent. In this respect, the Eh of the Candiota surface waters within piles, pit lakes, and streams extend over a large range. In waste piles, water should be in equilibrium with the atmosphere. In the pit lakes, however, measured Eh potentials in the range of 650–700 mV indicate values less than atmospheric equilibrium. At acidic pH (2.2–3.3), such potentials correspond to oxygen partial pressures (pO_2) in the range of 10^{-26} to 10^{-27}, significantly less than the pO_2 in the atmosphere (0.2 atm or $10^{-3.7}$). Such values suggest an important decrease in O_2 partial pressure extending close to

the lake's surface. Modeling shows that in these conditions, the dissolved Fe is mainly Fe(II) in pit lake waters and some piles. In these cases, Fe(II) mainly consisted of Fe^{2+} and $FeSO_4$ species. Fe(III) content was only 1/100, 1/20, and 1/10 of the Fe(II) in the P4A-a, L4A-a, and L4A-b samples, respectively. Fe(III) mainly consisted of $Fe(OH)^{2+}$, $Fe(OH)_2^+$, and Fe^{3+}species.

These results explain major features of the surface waters and in particular the pit lake environment. Bottom lake sediments are grey to green, with no apparent sign of Fe^{3+}-bearing precipitates. XRD analyses confirmed this observation. A progressive decrease in O_2 partial pressure with depth may exist, leading to destabilization of iron oxyhydroxides/hydroxysulfates that may be formed close to the surface, indicated by slightly positive or slightly negative SI values. A small increase in pH might result from this destabilization and would explain the presence of detrital mica in bottom lake sediment. The MCSSW normalized spectra of bottom lake material was compositionally consistent with that of residual materials after selective departure of calc-alkali and alkali elements (Ca, Mg, Na, and K).

The increased stability of Fe(III) minerals (hydroxysulfates/hydroxides) with the O_2 partial pressure correctly explains the presence of precipitates found in the drainage from waste piles and streams affected by AMD. In these two last environments, the deposits display magnificent ochre and dark red colors. Schwertmannite is commonly found in oxidic conditions, i.e. within the piles and at the pit lake discharges, as observed at many AMD sites (Bigham et al. 1996). However, schwertmannite is metastable and transforms to goethite through aging (Bigham et al. 1996) and under anoxic conditions (Burton et al. 2008). Along with the difficulty of using XRD to detect schwertmannite, the metastability of this mineral may also explain why it was not observed, unlike goethite, which was observed. Oxidic conditions should also explain the presence of goethite in BLD-L1A-II. This sample is a deposit from a bottom rock located close to the edge of a pit lake, indicating that this rock is exposed from time to time in dry weather.

Finally, these modeling results explain that the general Fe deficit of the surface waters is the consequence of scavenging of this element in Fe sulfate salts, hydroxysulfate, and oxyhydroxide precipitates in the waste piles and in O_2-rich waters at the surface of the lakes and thereafter in streams at the pit lake outlets.

Steady pH of 2.7–3 of the Pit Lake Waters

Geochemical modeling was used to assess the reaction pathways by which the pit lakes and piles acquire their chemical features: in particular, a steady pH of 2.7–3 in the lake without substantial precipitation of iron hydroxides. Several modeling pathways were tested and the results showed that the carbonate/sulfur dissolution ratio is the key parameter constraining pH. When calcite dissolves more extensively than pyrite, it buffers the pH at alkaline values, leading to gypsum and ferrihydrite precipitation. In the absence of carbonates, or if they dissolve more slowly than pyrite oxidizes, ferric iron is produced; subsequent hydrolysis leads to a continuous drop in pH. In the intermediate case when calcite and pyrite react on the same order of magnitude, the aqueous carbonate system counterbalances protons produced by pyrite oxidation. The low pH is due to the buffering of species involving sulfate (SO_4/HSO_4^-, pK = 1.4) and iron oxyhydroxides (Fe^{3+}/FeOOH, $Fe^{3+}/Fe(OH)_2^+$, $Fe^{3+}/Fe(OH)_3$ with pK values of 1.98, 2.4, and 3.3, respectively). Introduction of additional silicate phases (albite, K-feldspar) is associated with a slight increase in pH, to 2.7–3.3, due to proton/cation exchange during hydrolysis of these phases. These calculations show that the lake chemistry can be explained by the concomitant dissolution of pyrite and carbonate phases in some proportion, the additional dissolution of a few silicate phases, and the buffering of Fe oxyhydroxide species.

Pit Lake Water Compositional Evolution with Age: Lakes as Opened Reactors Systems

An interesting evolution of the chemical water compositions of the pit lakes with their relative age of formation was observed. From the most recent pit lakes (lake IV) to the intermediate (lake II), and the oldest (lake I), there was a significant decrease of SO_4 content and an associated decrease in major cations (Fig. 5). To interpret this evolution, we must recall that the lakes represent a reservoir periodically filled with rain, and have an open outflow. Thus, they can be considered an open-flow reservoir. The observed evolution may be interpreted as due to progressive evolution of the mineralogical composition of the altered rocks through dissolution of the most soluble phases as pyrite and carbonates, and a decreased reaction rate due to the coating of mineral surfaces with time.

The solid materials found on the lake bottom display characteristics of residual materials. They actually are mainly composed of residual mineral phases left after alteration. This residual nature is consistent with advanced interpretations regarding lakes as open reactor systems that consider their evolution through time.

Modeling

To support these interpretations, the quantitative results of a simple model of dissolution/precipitation using the geochemical modeling computer code PHREEQC were allowed to fit the composition of pit lake water L4A-b, taken

Table 2 Results of a dissolution/precipitation model for the genesis of the Candiota waters, fitting the composition of a pit lake water sample (L4A-b)

Phases	Dissolved/precipitated (mmol)	(%)	Chemical composition							
			Dissolved or precipitated chemical components (μmol)							
			SiO_2	SO_4^-	Ca^{++}	Mg^{++}	Na^+	K^+	Al^{+++}	Fe, T
Dissolved										
Pyrite	9.2	42.0		18.4						9.2
Calcite	4	18.3			4.0					
Dolomite	4.4	20.1			4.4	4.4				
Albite	2.4	11.0	7.2				2.4		2.4	
K-feldspar	1.9	8.7	5.7					1.9	1.9	
	Total	100								
Precipitated										
Goethite	6.9	33.2								6.9
K-jarosite	0.75	3.6		1.5				0.8		2.3
Alunite	0.75	3.6		1.5				0.8	2.3	
Gypsum	0.4	1.9		0.4	0.4					
Quartz	11.13	53.6	11.1							
Kaolinite	0.85	4.1	1.7						1.7	
	Total	100								
Water budget			0.07	15.0	8.0	4.4	2.4	0.40	0.35	0.05
L4B-b sample			0.07	14.9	8.0	4.5	2.4	0.41	0.38	0.07
% of Components precipitated in secondary phases			99.5	18.5	4.8	0.0	0.0	78.9	91.9	99.5

as an example in Supplemental Table 1. The model presented in Table 2 accounts for the main points raised about the major element compositional characteristics of the Candiota surface waters.

1. Preferential dissolution of pyrite and calcite/siderite (more generally Ca/Mg carbonates) was assumed. These phases represent 80.4 % of the dissolved phases (in moles), and their dissolution is the cause of the elevated SO_4, Ca, and Mg content of the surface water. The dissolution of additional silicate phases encompass albite (11 % of the dissolved phases), which accounts for the Na, and K-feldspar (8.7 % of the dissolved phases), which contributes the K for jarosite and alunite precipitation;
2. The proportion of dissolution of carbonate over sulfur was fixed near 0.9 in this model. This proportion induces pH values of approximately 2.7 for surface solutions;
3. Along the evolution of the surface water, the only sulfate-bearing phases assumed to precipitate were jarosite and alunite in a very low proportion of the precipitating phases (each representing 3.6 %), and gypsum in an even lower proportion (1.9 %). The precipitation of these phases consumes only 18.5 % of dissolved sulfate. Without any significant precipitation of Ca, Mg, and SO_4-bearing phases, the model accounts for the global Ca, Mg, and SO_4 correlation observed in the pit lake waters;
4. Modeling results indicate that Fe almost entirely precipitates as the water evolves at the surface. SI calculations and mineralogical observations both indicate that jarosite and goethite are the two ultimate Fe-bearing precipitates. This is consistent with these two minerals being more stable than schwertmannite and ferrihydrite in AMD (Bigham et al. 1996). Through analysis of numerous discharge waters from abandoned coal mines in Pennsylvania in log(Fe) versus pH and Eh–pH diagrams (with values consistent with those of Candiota waters), Cravotta (2008) also concluded that jarosite and goethite should limit Fe stability in the low pH range. In our modeling, goethite precipitation accounts for 75 % of the Fe depletion in surface solutions. The remaining percentage is related to Fe-sulfate bearing phases (jarosite precipitation);
5. Al solubility was assumed to be limited by precipitation of alunite (Al- and SO_4-bearing phase) and kaolinite (Al- and SiO_2-bearing phase). This choice differs from Cravotta (2008), who favored precipitates of jurbanite ($Al(SO_4)(OH)5H_2O$) for the Al- and SO_4-bearing phase, and allophane ($1\text{-}2SiO_2\ Al_2O_3\ 5\text{-}6H_2O$)

for the Al- and SiO_2-bearing phase in AMD from abandoned coal mines. However, in Candiota, these phases were not observed, while kaolinite was commonly observed, particularly in the lake bottom deposits. As advanced previously, the presence of kaolinite would also probably indicate some pH increase at the lake bottom;

6. The prediction for the modeled solution obtained after dissolution/precipitation process with pH values close to 2.7-3 fits the L4A-b water sample composition well.

Interpretation of Groundwater Chemistry

Groundwater displays distinctly different geochemical characteristics from surface water. Bicarbonate becomes more and more dominant as pH increases, with the most significant increase occurring in the pH range of 6.2–6.5. This evolution indicates that pyrite oxidation is no longer the major process controlling pH. In fact, groundwater pH is controlled by the carbonate/bicarbonate system. This carbonate/bicarbonate control should be promoted by high pCO_2 levels originating from the decomposition (partial oxidation) of organic matter present in the vadose zone or coming from coal seams and the concurrent dissolution of carbonate minerals in the Rio Bonito Formation. Limited degassing of these subterraneous levels maintains high CO_2 pressure.

Groundwater also displays significantly lower cation and anion concentrations than surface water. In the MCSSW-normalized spectra (Fig. 8), groundwater is distinguished from pit lake water by a lower compositional range. Among the major 'soluble' cations, Na and K only partly recover the compositional range of pit lake solutions, and Ca and Mg are more significantly depleted. There is very significant depletion of Fe, Al, and Ga. SiO_2 is the only constituent whose content resembles that in the pit lakes. This is indicative of and consistently explained by alteration rates and evolution of water compositions in aquifers being significantly different from surface conditions. Lower O_2 partial pressure within an aquifer leads to lower alteration rates, explaining the lower content of 'soluble' elements (SO_4, Ca, Mg, Na, K). The low Fe and Al content in groundwater compared to surface water is explained by the lower solubility of these elements at higher pH, as clearly apparent in the classical solubility versus pH curves for these elements. In contrast, the solubility of SiO_2 does not vary much with pH, explaining similar levels of this element in ground and surface water.

PHREEQC modeling indicates differences in the evolution of surface and ground waters as a consequence of distinct physico-chemical conditions. As in the surface conditions, substratum phase minerals (calcite, pyrite, albite, and plagioclase) remain undersaturated in aquifer conditions and thus susceptible to dissolution. The assemblage of saturated phases susceptible to precipitate as groundwater evolves, based on geochemical modeling, is different from the saturated phases assemblage susceptible to precipitate in surface water. According to the geochemical model, iron oxyhydroxides/oxides (goethite, hematite) remain oversaturated till very low O_2 pressure conditions. These phases are observed in sandstone samples from aquifer cores. Iron and aluminum hydroxysulfates, like jarosite and alunite, are not stable in neutral pH groundwater. Barite and gypsum constitute the prevalent sulfate-bearing phases susceptible to precipitation. Gypsum is slightly undersaturated in most waters but may precipitate in some SO_4- and Ca-rich waters, explaining its presence in some sandstone samples. At neutral pH, some clay minerals (kaolinite, montmorillonite, illite, and smectite) become stable.

Conclusions

Surface and ground water display distinct compositional characteristics in the Candiota area. Analyses of these characteristics constrain the modality of the alteration process at the origin of these waters and the further evolution of the waters at the surface through precipitation of specific phases. Normalization to the mean substratum rock composition helps explain the distribution of the elements, since normalized surface waters are SO_4-, Ca-, and Mg-enriched relative to their distribution in the mean substrata. These geochemical characteristics are the result of preferential pyrite oxidation and carbonate dissolution in a given proportion, pyrite and carbonate being diagenetic minerals in coal and sandstone above and below coal seams.

The waters are highly acidic (mean pH values 2.7–3) due to pyrite oxidation. High acidity favors hydrolysis of K-feldspar, plagioclase, and micas. The correlation between sulfate and Ca, Mg, and Na content in pit lake samples are a consequence of substrate dissolution without any significant precipitation of secondary phases that include these elements, while Al and Si content can be controlled by clay minerals (kaolinite). In agreement with model results, observations indicate that Fe hydroxysulfates/oxyhydroxides precipitate near the piles and in streams. A progressive decrease in O_2 partial pressure within pit lakes leads to destabilization of iron hydroxysulfates/oxyhydroxides, which explains their absence in lake sediment. A decrease in sulfate and major cation content with the relative age of the pit lakes is explained by these being open flow systems. Compositional evolution can be ascribed to progressive decrease in the weathering rate of the rocks in the lake with time, induced by

progressive dissolution of the most "soluble" minerals and coating of mineral surfaces.

Groundwater is characterized by low salinity and a slightly acidic to near-neutral pH, and is dominated by bicarbonates. This is the consequence of: (i) a limited supply of oxygen from the surface that restricts pyrite oxidation; (ii) pH control by the carbonate/bicarbonate system, promoted by high pCO_2 levels originating from the decomposition of organic matter, the concurrent dissolution of carbonate minerals, and limited degassing; (iii) hydrolysis of silicate minerals contributing to pH stabilization near neutral; and (iv) high adsorption rates of cations onto clay minerals (smectites in particular) and Fe oxyhydroxides (particularly goethite).

Acknowledgments The study was supported by the Brazilian National Research Council (CNPQ—research grant 472766/2003-1). The authors gratefully acknowledge Companhia Riograndense de Mineração (CRM) for logistical support and for allowing access to the well cores, sample materials, and the Candiota Mine.

References

Alpers CN, Blowes DW, Nordstrom DK, Jambor JL (1994) Secondary minerals and acid mine-water chemistry. In: Jambor JL, Blowes DW (eds) Environmental geochemistry of sulfide mine-wastes, mineral assoc Canada short course, vol 22, pp 247–270

Bigham JM, Nordstrom DK (2000) Iron and aluminum hydroxysulfates from acid sulfate waters. In: Alpers CN, Jambor JL, Nordstrom DK (eds) Sulfate minerals—crystallography, geochemistry, and environmental significance, Mineral Soc Amer 40, Washington, DC, USA, pp 351–403

Bigham JM, Schwertmann U, Traina SJ, Winland RL, Wolf M (1996) Schwertmannite and the chemical modeling of iron in acid sulfate waters. Geochim Cosmochim Acta 60:2111–2121

Braungardt CB, Achterberg EP, Elbaz-Poulichet F, Morley NH (2003) Metal geochemistry in a mine polluted estuarine system in Spain. Appl Geochem 18:1757–1771

Burton ED, Bush RT, Sullivan LA, Mitchell DG (2008) Schwertmannite transformation to goethithe via the Fe(II) pathway: reaction rates and implications for iron-sulfide formation. Geochim Cosmochim Acta 72:4551–4564

Casiot C, Morin G, Juillot F, Bruneel O, Personné J, Leblanc M, Duquesne K, Bonnefoy V, Elbaz-Poulichet F (2003) Bacterial immobilization and oxidation of arsenic in acid mine drainage (Carnoulès creek, France). Water Res 37:2929–2936

Casiot C, Egal M, Elbaz-Poulichet F, Bruneel O, Banco-Montigny C, Cordier M, Gomez E, Aliaume C (2009) Hydrological and geochemical control of metals and arsenic in a Mediterranean river contaminated by acid mine drainage (the Amous River, France); preliminary assessment of impacts on fish (Leuciscus cephalus). Appl Geochem 24:787–799

Correa da Silva ZC (1993) Candiota coal field: a world class Brazilian coal deposit. Int J Coal Geol 23:103–116

Cravotta CA III (2008) Dissolved metals and associated constituents in abandoned coal-mine discharges, Pennsylvania, USA. Part 2: geochemical controls on constituent concentrations. Appl Geochem 23:203–226

Daemon RF, Marques-Toigo M (1991) An interpreted biostratigraphic column for the Paraná Basin, Brazil. In: Proceedings of the international congress on carboniferous-permian geology and stratigraphy, Buenos Aires, Argentina

DNPM (2006) Brazilian mineral yearbook—part III: statistics by commodities. DNPM/MME. http://www.dnpm.gov.br/assets/galeriaDocumento/AMB2006/substancia%20a-e.pdf, Accessed June 2009

Dupre B, Gaillardet J, Rousseau D, Allegre CJ (1996) Major and trace element in river borne material: the Congo Basin. Geochim Cosmochim Acta 60:1301–1321

Edraki M, Golding SD, Baublys KA, Lawrence MG (2005) Hydrochemistry, mineralogy and sulfur isotope geochemistry of acid mine drainage at the Mt. Morgan mine environment, Queensland, Australia. Appl Geochem 20:789–805

Elbaz-Poulichet F, Morley NH, Beckers Cruzado A, Velazquez Z, Green D, Achterberg EP, Braungardt CB (1999) Trace metal and nutrient distribution in an extremely low pH (2.5) river estuarine system, the Ria El Huelva (south west Spain). Sci Total Environ 227:73–83

Elbaz-Poulichet F, Morley NH, Beckers JM, Nomerange P (2001) Metal geochemistry in a mine polluted estuarine system in Spain. Appl Geochem 18:1757–1771

Fiedler H, Solari J (1988) Caracterização do impacto ambiental da mina de Candiota sobre as águas superficiais da região. Anais do Encontro Nacional de Tratamento de Minérios e Hidrometalurgia, São Paulo, ABES, Brazil 13:483–498

Fiedler H, Martins AF, Solari J (1990) Meio ambiente e complexos carboelétricos: o caso de Candiota. Ciência Hoje 68:38–45

Gammons CH, Duaime TE, Parker SR, Poulson SR, Kennelly P (2010) Geochemistry and stable isotope investigation of acid mine drainage associated with abandoned coal mines in central Montana, USA. Chem Geol 269:100–112

Hammastrom JM, Seal RR, Meier AL, Kornfeld JM (2005) Secondary sulfate minerals associated with acid drainage in the eastern US: recycling of metals and acidity in surficial environments. Chem Geol 215:407–431

Holz M (1998) The Eo-Permian coal seams of the Paraná Basin in southernmost Brazil: an analysis of the depositional conditions using sequence stratigraphy concepts. Int J Coal Geol 36:141–163

Holz M, Kalkreuth W (2004) Sequence stratigraphy and coal petrology applied to the early permian coal-bearing rio bonito formation, Paraná Basin, Brazil. In: Pashin J, Gastaldo R (eds) Sequence stratigraphy, paleoclimate, and tectonics of coal-bearing strata, AAPG studies in geology vol 51, pp 147–167

Jambor JL (1994) Mineralogy of sulfide-rich tailings and their oxidation products. In: Jambor JL, Blowes DW (eds) Environmental geochemistry of sulfide mine-wastes, Mineral Assoc Canada Short Course vol 22, pp 59–102

Kalkreuth W, Holz M, Kern M, Machado G, Mexias A, Silva MB, Willet J, Finkelman R, Burger H (2006) Petrology and chemistry of Permian coals from the Paraná Basin: 1. Santa Terezinha, Leão-Butiá and Candiota coal fields, Rio Grande do Sul, Brazil. Int J Coal Geol 68:79–116

Ketzer JM, Holz M, Morad S, Al-Aasm IS (2003) Sequence stratigraphic distribution of diagenetic alterations in coal-bearing, paralic sandstones: evidence from the Rio Bonito Formation (early Permian), southern Brazil. Sedimentology 50:855–877

Machado JFL (1985) Mineração de carvão: contaminação e vulnerabilidade dos mananciais. Boletim de Resumos Expandidos do II Simpósio Sul-Brasileiro de Geologia, Florianópolis, SBG, Brazil 1:539–553

Machado JLF, Peruffo N, Luna JES (1984) Projeto de Estudo da Vulnerabilidade à Contaminação dos Mananciais Subterrâneos

Decorrente da Extração do Carvão Mineral. CPRM internal report

Martins AF, Zanella R (1987) Análise de águas de superfície e de profundidade da região de Candiota, RS: determinação da concentração de elementos traços de relevância ambiental, elementos menores e macroelementos. Proc Anais do I Congresso Brasileiro de Geoquímica, Porto Alegre, SBG, Brazil 2:217–223

Martins AF, Zanella R (1990) Estudo analítico-ambiental na região carboenergética de Candiota, Bagé (RS). Ciência e Cultura 42:264–270

Nicholson RV, Gillham RW, Reardon EJ (1988) Pyrite oxidation in carbonate-buffered solution: 1. experimental kinetics. Geochim Cosmochim Acta 52:1077–1085

Nicholson RV, Gillham RW, Reardon EJ (1990) Pyrite oxidation in carbonate-buffered solution: 2. Rate control by oxide coatings. Geochim Cosmochim Acta 54:395–402

Nordstrom DK, Alpers CN (1999) Negative pH, efflorescent mineralogy, and consequences for environmental restoration at the Iron Mountain Superfund site, California. Proc Natl Acad Sci USA 96:3455–3462

Pankhurst DL, Appelo CAJ (1999) User's guide to PHRE-EQC (version 2)—a computer program for speciation, batch-reaction, one-dimensional transport, and inverse geochemical calculations. USGS WRI Rept 99-4259, Washington DC, USA

Patzkowsky ME, Smith LH, Markwick PJ, Engberts CJ, Gyllenhaal (Ed) (1991) Application of the Fuijita-Ziegler paleoclimatic model: early Permian and late Cretaceous examples. Palaeogeogr, Palaeoclimatol, Palaeoecol 86:67–85

Pérez MA, Moreira-Turcq P, Gallard H, Allard T, Benedetti MF (2011) Dissolved organic matter dynamic in the Amazon basin: sorption by mineral surfaces. Chem Geol 286:158–168

Pires M, Querol X (2004) Characterization of Candiota (South Brazil) coal and combustion byproducts. Int J Coal Geol 60:57–72

Salomons W (1995) Environmental impact of metals derived from mining activities: processes, predictions, prevention. J Geochem Explor 52:5–23

Sánchez España J (2007) The behavior of iron and aluminum in acid mine drainage: speciation, mineralogy, and environmental significance. In: Letcher TM (ed) Thermodynamics, solubility and environmental issues. Elsevier, Amsterdam, pp 137–150

Sánchez España J, López Pamo E, Santofimia E, Aduvire O, Reyes J, Barettino D (2005a) Acid mine drainage in the Iberian Pyrite belt (Odiel River watershed, Huelva, SW Spain): geochemistry, mineralogy and environmental implications. Appl Geochem 20:1320–1356

Sánchez España J, Lopez Pamo E, Santofimia Pastor E, Reyes Andres J, Martin Rubi J (2005b) The natural attenuation of two acidic effluents in Tharsis and La Zarza-Perrunal mines (Iberian Pyrite Belt, Huelva, Spain). Environ Geol 49:253–266

Sánchez España J, Yusta I, Diez-Ercilla M (2011) Schwertmannite and hydrobasaluminite: a re-evaluation of their solubility and control on the iron and aluminium concentration in acidic pit lakes. Appl Geochem 26:1752–1774

Stallard RF, Edmond JM (1983) Geochemistry of the Amazon: 2. the influence of geology and weathering environment on the dissolved load. J Geophys Res 88:9671–9688

Streck CD (2001) Estudo da qualidade das águas superficiais e estimativa dos fluxos de elementos-traço na região de Candiota, RS. Diss, Pontifícia Universidade Católica do Rio Grande do Sul, Brazil

Taylor SR, McLennan SM (1985) The continental crust: its composition and evolution. Blackwell, Oxford, UK

Teixeira EC, Sanchez JCD, Migliavacca D, Binotto R, Fachel JMG (2000) Environmental assessment: study of metals in fluvial sediments in sites impacted by coal processing and steel industry activities. Fuel 79:1539–1546

Tosiani T, Loubet M, Viers J, Valladon M, Tapia J, Marrero S, Yanes C, Ramirez A, Dupre B (2004) Major and trace elements in river-borne materials from the Cuyuni basin (southern Venezuela): evidence for organo-colloidal control on the dissolved load and element redistribution between suspended and dissolved load. Chem Geol 211:305–334